RESEARCH ARTICLE

Turning 3D Covalent Organic Frameworks into luminescent ratiometric temperature sensors

Laurens Bourda[1,2], Anna M. Kaczmarek[3]*, Min Peng[1], Sonali Mohanty[3], Hannes Rijckaert[4], Pascal Van Der Voort[2], Kristof Van Hecke[1]*

[1] XStruct, Department of Chemistry, Ghent University, Krijgslaan 281-S3, Ghent, Belgium
[2] Center for Ordered Materials, Organometallics and Catalysis (COMOC), Department of Chemistry, Ghent University, Krijgslaan 281-S3, Ghent, Belgium
[3] NanoSensing Group, Department of Chemistry, Ghent University, Krijgslaan 281-S3, Ghent, Belgium
[4] SCRiPTS, Department of Chemistry, Ghent University, Krijgslaan 281-S3, Ghent, Belgium
* Corresponding authors, E-mail: anna.kaczmarek@ugent.be; kristof.vanhecke@ugent.be

Supporting information for this article is given via a link at the end of the document.

Abstract We report on hybrid crystalline lanthanide-containing 3D Covalent Organic Framework (Ln@3D COF) materials for temperature sensing applications. Two different synthesis methodologies were used. In a first approach, a bipyridine-containing 3D COF (Bipy COF) was grafted with a range of visible emitting lanthanide (Eu^{3+}, Tb^{3+}, Dy^{3+} and Eu^{3+}/Tb^{3+}) β-diketonate complexes. In a second approach, a novel nanocomposite material was prepared by impregnating a 3D COF without available coordination sites (COF-300) with upconverting $NaYF_4$:Er,Yb nanoparticles. To the best of our knowledge, the developed luminescent materials here are the first 3D COFs to be tested as ratiometric temperature sensors. In fact, for the Bipy COF, two different types of thermometers were tested, including a rare Dy^{3+} system, showing excellent temperature sensing properties, while the $NaYF_4$:Er,Yb@COF-300 material combines upconverting nanoparticles with 3D COFs. As such, our findings open a new pathway towards potentially multifunctional materials which can combine thermometry with other modalities e.g. catalysis or drug delivery.

Introduction

Covalent Organic Frameworks (COFs)[1] are prepared as highly stable and crystalline permanently porous materials using the principles of dynamic covalent chemistry.[2,3] COFs are also highly designable as the functional groups and pore sizes can be tuned by reticular chemistry. COFs have been used in several application fields already, including catalysis, gas sorption, separation and storage and drug delivery.[4-11] Until now, most of the COF research has been focused on two-dimensional (2D) COFs, as those are easier to obtain in crystalline form.[12] However, due to the shift from weak interlayer interactions to fully covalently bonded materials, three dimensional (3D) COFs are highly interesting.[2,3] Moreover, the structural diversity of 3D COFs is far higher, even enlarging the designability of these materials. Additionally, these 3D COFs can be further functionalized, for instance by grafting of metal complexes[13,14] or by impregnating clusters and nanoparticles (NPs).[15,16]

Trivalent lanthanide ions (Ln^{3+}) are well studied for their luminescent properties, owing to their shielded 4f-4f transitions and resulting in narrow emission, long decay times and high quantum yields.[17,18] To overcome their low absorption coefficients, lanthanide ions are typically combined with a ligand which can be used to excite the ions (the so-called antenna effect). Recently, lanthanide materials, including hybrid materials, have been explored as thermometers, where the well separated lanthanide emission peaks afford an ideal scaffold for ratiometric temperature sensing.[19-27] This allows measurement of temperature in a non-invasive way, independent of external factors, as all peaks are affected equally. Ratiometric luminescence thermometers have already found a wide range of exciting applications, such as employing them to measure temperature in the human body to detect cancer cells, in catalytic reactors to optimize the yield of the reaction in the reactor beds, or to map elevated temperatures in microelectronics.[28-30]

Among the various explored materials, Metal Organic Frameworks (MOFs) and recently also 2D COFs have been used to accommodate Ln^{3+} ions and Ln^{3+} complexes and were further explored as temperature sensors. Most often, this is achieved by grafting of Ln^{3+} ions to the COF/MOF materials.[22-24] Additionally, lanthanide-doped upconversion nanoparticles (UCNPs) have recently been impregnated in MOFs for in-situ temperature measurement during a MOF-catalyzed reaction.[27] Also UCNPs and 2D COFs have already been combined in a core-shell material (where the UCNPs are the cores and the 2D COFs form the shells), developing advanced nanoplatforms for simultaneous catalysis and thermometry.[25]

However, 3D COFs, although a very interesting class of COF materials, have scarcely been explored for combination with lanthanides. Up to date, there is only one report of a 3D COF grafted using a Eu^{3+} salt ($Eu(NO_3)_3 \cdot 6H_2O$) for use as a chemosensor for quinones.[31] Additionally, to the best of our knowledge, no work has been reported on the use of 3D COFs as thermometers or the combination of COFs with lanthanide NPs. In general, there have previously been no reports of COFs impregnated with lanthanide NPs, analogous to what is already known to be possible for MOFs.[27] In fact, the only known COF-inorganic NP hybrid materials are those where an inorganic NP is the core and the 2D COF forms a shell as stated above.[25]

In this work, we aimed at developing hybrid Ln@3D COF materials which would be suitable for temperature sensing applications. To achieve this, several different routes were investigated, i.e. two different 3D COFs were prepared, a bipyridine 3D COF (Bipy COF) and a non-functionalized 3D COF (COF-300). Bipy COF, which has available N-coordination sites, was grafted with different ratios of Ln^{3+}-β-diketonate (acetylacetone, acac) complexes. In another approach, COF-300, selected as a COF without readily available coordination sites, was synthesized and further used to prepare a nanocomposite with $NaYF_4$:Er,Yb UCNPs impregnated in the COF host surface.

Both approaches yield strongly emitting luminescent materials suitable for
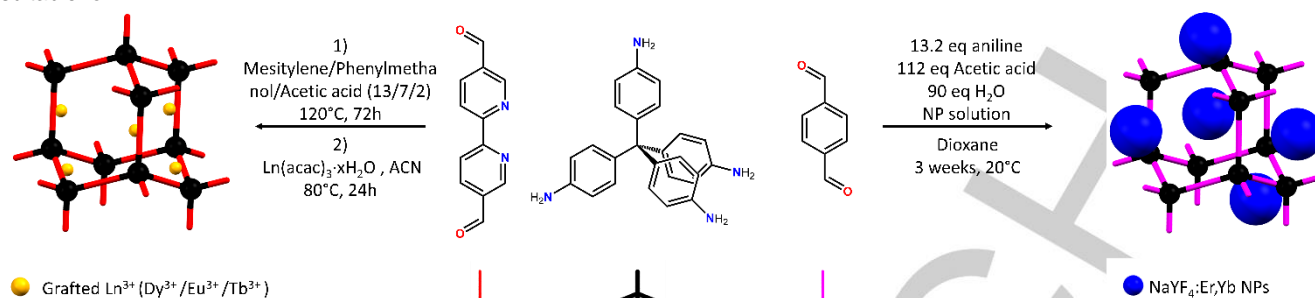

Scheme 1. Schematic representation of the synthesis of Ln³⁺-grafted Bipy COF and UCNP impregnated COF-300.

thermometric applications, further studied in detail in this work. The proposed here 3D COF-based materials could potentially find interesting applications as biological thermometers or combined catalysis-thermometry applications as shown in some of our earlier works on lanthanide 2D COF hybrid materials and lanthanide MOF nanocomposites.[23-25,27,32] The combination of a porous COF material with a luminescent lanthanide emitter (NP or complex) gives room to moving towards multifunctional applications e.g. combining thermometry with drug delivery. In general, the use of 3D COFs is highly beneficial, because of their unique porous features in terms of ordered pore structure and excellent performances compared to 2D frameworks. This rich structural diversity, in terms of high surface areas, low densities, tunable pore size and shape and abundant easily accessible active sites, is particularly attainable through 3D COFs.

Results and Discussion

The synthetic approaches employed to develop the studied materials are summarized in **Scheme 1**. Bipy COF was synthesized, using a previously reported procedure,[33] in a mesitylene/phenylmethanol/acetic acid mixture set at 120 °C. Afterwards, the resulting material was mixed with $Ln(acac)_3 \cdot xH_2O$ complexes (Ln = Dy^{3+}, Eu^{3+}, Tb^{3+}) in acetonitrile (ACN) for 24 h at 80 °C to obtain Eu@Bipy COF, Tb@Bipy COF Dy@Bipy COF and Eu,Tb@Bipy COF. Analysis of the pristine Bipy COF using powder X-ray diffraction (PXRD) showed typical peaks at 2θ = 5.1, 7.5, 15 and 21.5° (**Figure 1A**) matching with the (200), (220), (321) and (820) Bragg reflections, respectively, of the modelled structure as previously reported by Sun *et al.*[32] Furthermore, to check the effect of the Ln^{3+} complex grafting on the COF structure, samples grafted with three different amounts (1, 2 and 4 equivalents) of $Eu(acac)_3 \cdot xH_2O$ were analyzed with PXRD. While some reduction in crystallinity is observed, especially for the (4 eq.)-Eu@Bipy COF sample (as shown in red), the major peaks at 2θ = 7.5, 15 and 21.5° are still clearly observable as well as two unidentified new peaks at 19 and 29.5°. It must be noted that the missing (200) reflection at 5° is indicative for the internal order of the COF walls (as shown in **Figure S30**), while the retained (220) reflection is associated with the ordering of the porous COF network. The combination of lowered crystallinity with a disappearing reflection related to the internal order of the COF walls is indicative to partial COF linkage deformation by Ln^{3+} grafting and in agreement with earlier reports.[22,23] Additionally, the retention of higher order reflections as (220), (321) and (820) shows that the ordered COF structure did survive this post-
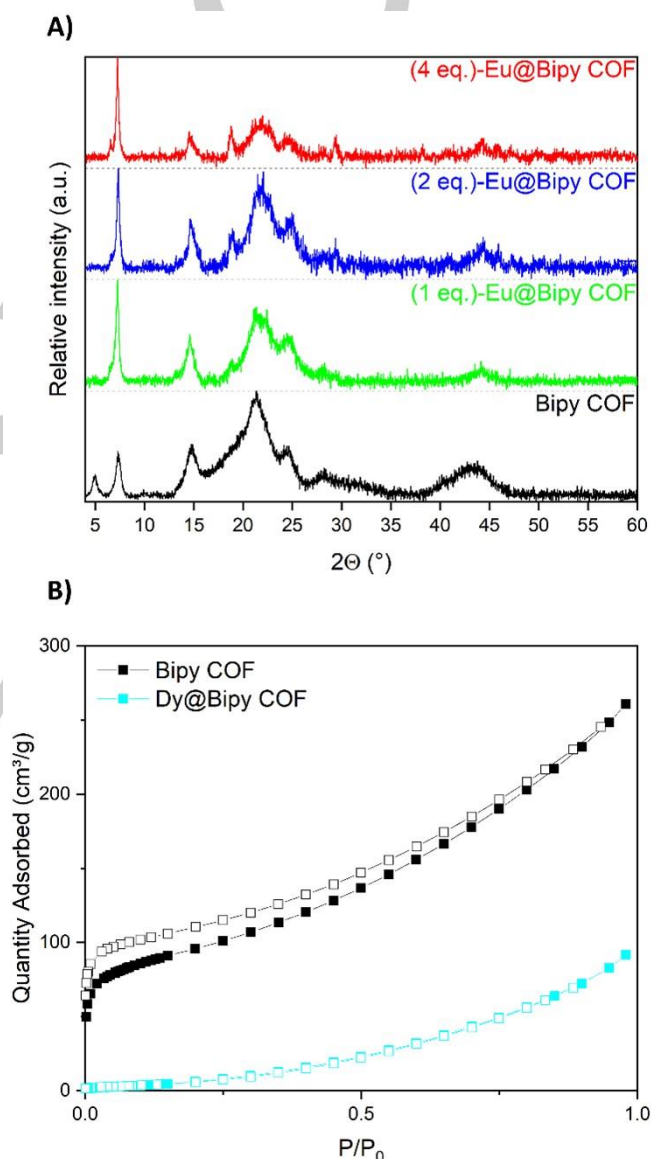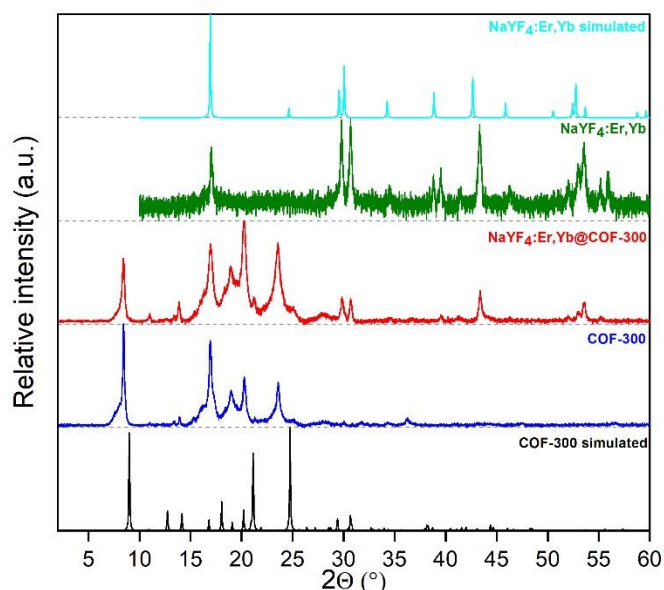

Figure 1. A) Background corrected PXRD patterns of pristine Bipy COF (black), (1 eq.)-Eu@Bipy COF (green), (2 eq.)-Eu@Bipy COF (blue) and (4 eq.)-Eu@Bipy COF (red). B) N_2-sorption isotherms for pristine Bipy COF (black) and Dy@Bipy COF (cyan).

modification reaction. To further confirm the successful grafting of the Ln^{3+} complexes, N_2 adsorption/desorption isotherms of one of the developed materials used for temperature sensing (Dy@Bipy COF, prepared using 4 equivalents of $Dy(acac)_3 \cdot xH_2O$) were obtained. A clear reduction in Brunauer-Emmett-Teller (BET)

surface area of the materials (the relevant N_2 adsorption/desorption isotherms at 77 K are presented in **Figure 1B**) is noticed from 350 m²/g for the pristine Bipy COF to only 20 m²/g for Dy@Bipy COF. Indeed, these results suggest the inclusion of additional heavy atoms and blocking of the micropores by the grafted lanthanides.[8,21,22,24] As no coordination sites are present in COF-300, another approach had to be taken to create the hybrid Ln@COF-300 nanocomposite materials. A first attempt to incorporate NaYF$_4$:Er,Yb UCNPs was performed by soaking COF-300 powder in an aqueous solution of Y(CF$_3$COO)$_3$, Yb(CF$_3$COO)$_3$, Er(CF$_3$COO)$_3$ and CF$_3$COONa at appropriate ratios and further heat-treating it to obtain NaYF$_4$:Er,Yb@COF-300. Kaczmarek *et al.* have previously used such approach to grow inorganic NPs in various (organo)silica-based materials.[34,35] We wanted to explore if this could be a successful route also for COF materials. However, analysis using high-angle annular dark-field scanning TEM (HAADF-STEM) with energy dispersive X-ray analysis (EDX) mapping (**Figure S4**) showed the COF was covered with a layer of NaYF$_4$:Er,Yb, rather than single NPs. Additionally, PXRD analysis (**Figure S5**) showed only NaYF$_4$:Er,Yb reflections were observed. Therefore, an alternative approach based on previously published NP@MOF research, where the MOF is grown in-situ in the presence of pre-synthesized NPs, was attempted.[27] However, in a first trial, compared to a pristine COF synthesized via the conventional route (COF-300_C), no significant difference with the sample with added UCNPs (NaYF$_4$:Er,Yb@COF-300_C) could be observed in TEM imaging (**Figure S7**). This can be explained due to the instantaneous precipitation of the COF upon addition of the catalyst, leaving no time for the nanocomposite material to form.[2] Therefore, the growth and precipitation of the COF crystals needed to be slowed down. This was achieved using a strategy to create COF-300 single crystals.[36] We opted for the synthetic protocol using an acetic acid/H$_2$O mixture as additive to which a 1,4-dioxane solution of the NaYF$_4$:Er,Yb NPs was added. This solution was then mixed with a solution of terephthalaldehyde and 13.2 eq. of aniline in 1,4-dioxane, subsequently sonicated and finally a solution of tetra-(4-anilyl)-methane (TAM) in 1,4-dioxane was added. The resulting NaYF$_4$:Er,Yb@COF-300 was slowly crystallized over three weeks at room temperature and was decanted and dried overnight at 80 °C in a vacuum oven before usage. PXRD analysis (**Figure 2**) of the resulting material (in red) shows the combination of strong COF reflections and weak NaYF$_4$:Er,Yb reflections, suggesting the formation of a hybrid material. The observed reflections match with pristine COF-300 (blue, synthesized via the same protocol without NaYF$_4$:Er,Yb UCNP addition) and NaYF$_4$:Er,Yb NPs (dark green), as well as simulated COF-300 (black, from the single crystal structure as published by Ma *et al.*[37]) and NaYF$_4$:Er,Yb (cyan, from ICSD PXRD data[38]). Additionally, the effect of NaYF$_4$:Er,Yb NP loading on the porous structure of COF-300 was checked using Ar-sorption at 87 K, the obtained results are presented in **Figure S11**. Although the obtained porosities are very low, this is in agreement with the results obtained in the initial report for the used procedure.[36] Despite the low porosity, it is still clear that, like in the previously discussed Dy@Bipy COF material, loading these crystals with NaYF$_4$:Er,Yb NPs decreased the Ar-uptake significantly.


Figure 2. Background corrected PXRD Patterns of NaYF$_4$:Er,Yb as simulated (cyan, ICSD 51916[38]) and obtained experimentally (dark green), NaYF$_4$:Er,Yb@COF-300 (red), COF-300 (blue) and COF-300 as simulated (black, from CCDC 1846136[37]).

Next, Scanning Electron Microscopy (SEM) images were taken to study the morphology of the materials (**Figure 3**). On the one hand, both COFs showed regular shape and particles of nanosize with especially COF-300 showing highly uniform particles, similar to the ones obtained for COF-300_C via the conventional synthesis (**Figure S3**). On the other hand, the Bipy COF particles are highly aggregated forming rod-like structures.
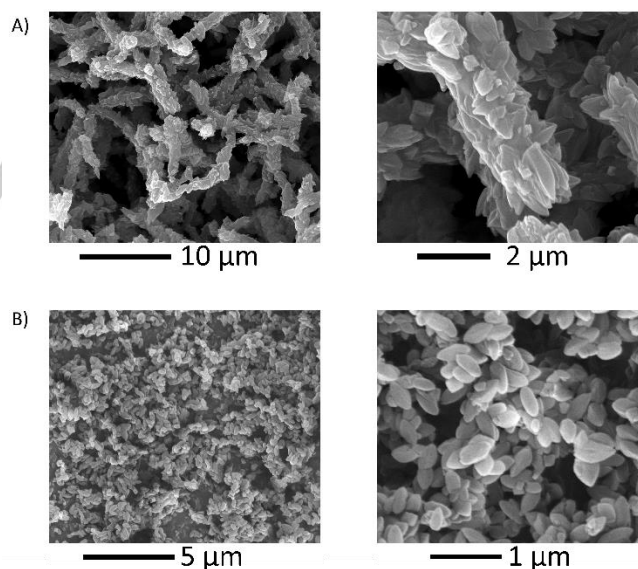
Figure 3. SEM images of: A) Bipy COF; B) NaYF$_4$:Er,Yb@COF-300.

Furthermore, distribution of the lanthanides over the COF materials was checked using HAADF-STEM, element maps of C, N, F, Na, Y, Tb, Er and Yb were obtained by EDX mapping. As expected, the presented results show a uniform spread of Tb^{3+} ions over the Tb@Bipy COF material (**Figure 4A**) indicating homogeneous lanthanide grafting. In contrast, in the NaYF$_4$:Er,Yb@COF-300 sample (**Figure 4B**) a clear distinction
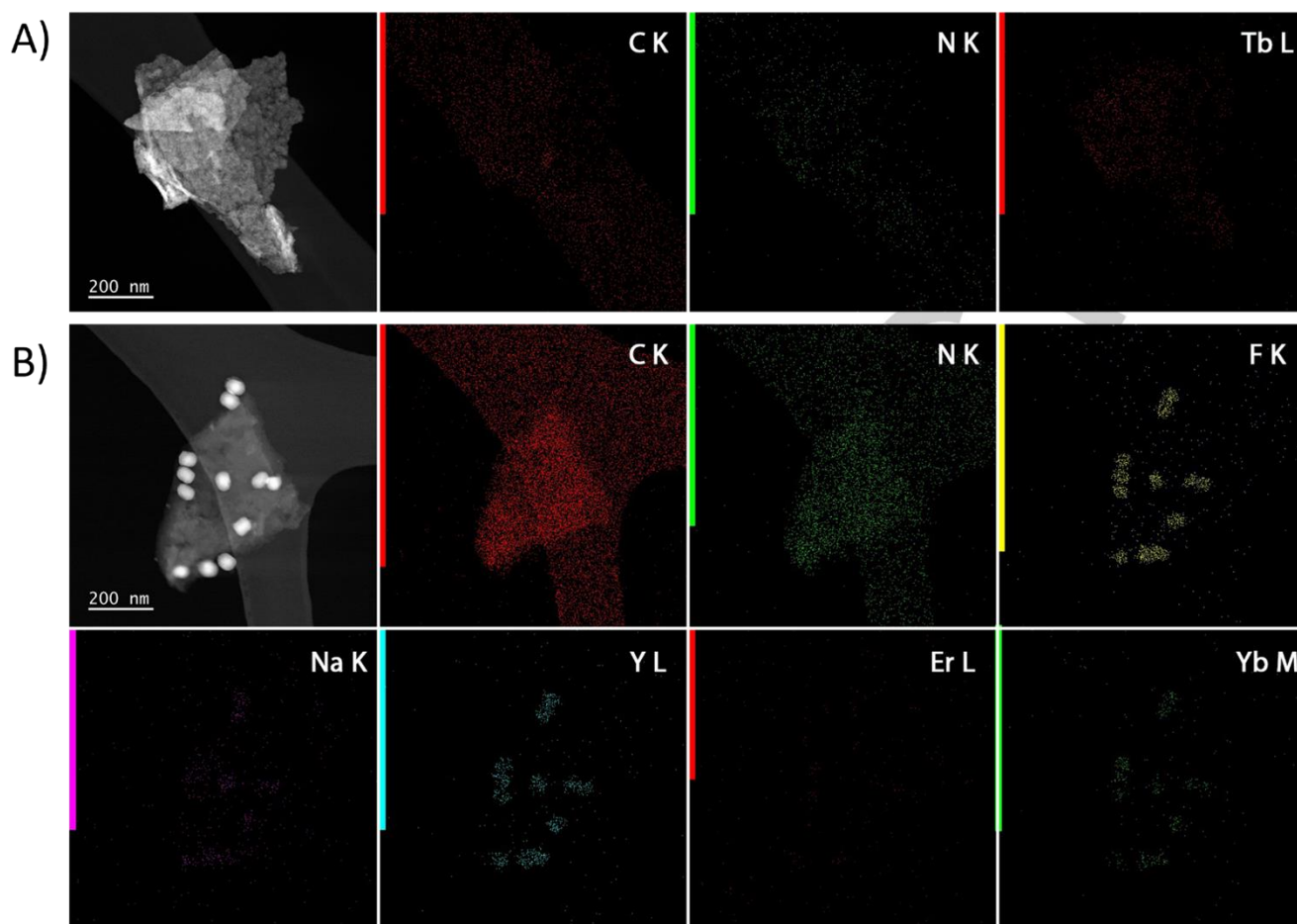
Figure 4. HAADF-STEM with EDX maps of A) Tb@Bipy COF and B) NaYF4:Er,Yb@COF-300 after PBS soaking. The following elements were mapped: A) C, N, Tb; B) C, N, F, Na, Y, Er, Yb.

can be made between the COF-300 particles (in the size range of a few hundreds of nm), showing high concentrations of C and N, and the NaYF$_4$:Er,Yb NPs on the surface of the COF, which appear much brighter and where mainly F and Y can be observed but also Na and Yb are clearly present. It should be noted that the initial shape of these NaYF$_4$:Er,Yb NPs was retained during the loading on the COF (**Figure S6**). Additionally, the stability of the composite material was confirmed by comparison of a HAADF-STEM with EDX mapping before (**Figure 4B**) and after a 24 h soaking step in phosphate-buffered saline (PBS, pH = 7.4, **Figure S9**), which shows no significant differences between both nanocomposites.

The photoluminescence (PL) properties of pristine Bipy COF were recorded at room temperature and are shown in **Figure S12**. In the excitation spectrum a broad band in the 300-450 nm range can be observed, with a maximum at around 341 nm. Upon exciting into this peak maximum, an emission band between 400-550 nm is obtained (maximum at 450 nm). As described above the Bipy COF material was further grafted with different Ln(acac)$_3$·xH$_2$O complexes (where Ln = Eu^{3+}, Tb^{3+}, Dy^{3+} or Eu^{3+}/Tb^{3+}) and the luminescence properties of these Ln@COF materials were studied. Here, lanthanide β-diketonate complexes were selected for grafting of the 3D COFs, instead of lanthanide salts, in order to provide a secondary ligand, which would work both as an antenna ligand, and to protect the lanthanide ions from

quenching by water molecules. The acetylacetone (acac) ligand was selected, as it has a high triplet level (25300 cm^{-1}),[22] which makes it a suitable ligand for lanthanides with a high accepting energy level, such as Tb^{3+} or Dy^{3+}.

In **Figure S13**, the excitation (A) and emission (B) spectra of the Eu@Bipy COF materials using increasing Eu^{3+} to COF ratios are shown. As the shape of the excitation spectra does not change significantly upon increase of grafted Eu^{3+}, it can be concluded that the material is unaltered upon Eu^{3+} coordination. Additionally, even though the Bipy COF emission band is highly prominent in the (1 eq.)-Eu@Bipy COF, the characteristic $^5D_0 \rightarrow ^7F_{0-4}$ transition peaks of Eu^{3+} can already be observed in this sample.[39] In the (2 eq.)-Eu@Bipy COF sample, these sharp peaks become more pronounced with an almost complete disappearance of the COF emission band. As the luminescent intensity is strongest in the (4 eq.)-Eu@Bipy COF sample, this Ln^{3+} to COF ratio was further used for the preparation of the other luminescent materials. To investigate the influence of the Bipy COF and acac ligand on the luminescence of the final hybrid Ln@COF materials, also EuCl$_3$ was grafted to the Bipy COF in varying amounts. These results are presented in the SI (**Figure S14**) and show that the EuCl$_3$ salt alone upon grafting to the Bipy COF does not provide satisfactory PL properties, although the Eu^{3+} peaks are present in the spectra confirming their successful grafting to the COF. These results could be expected as the employed acac ligand
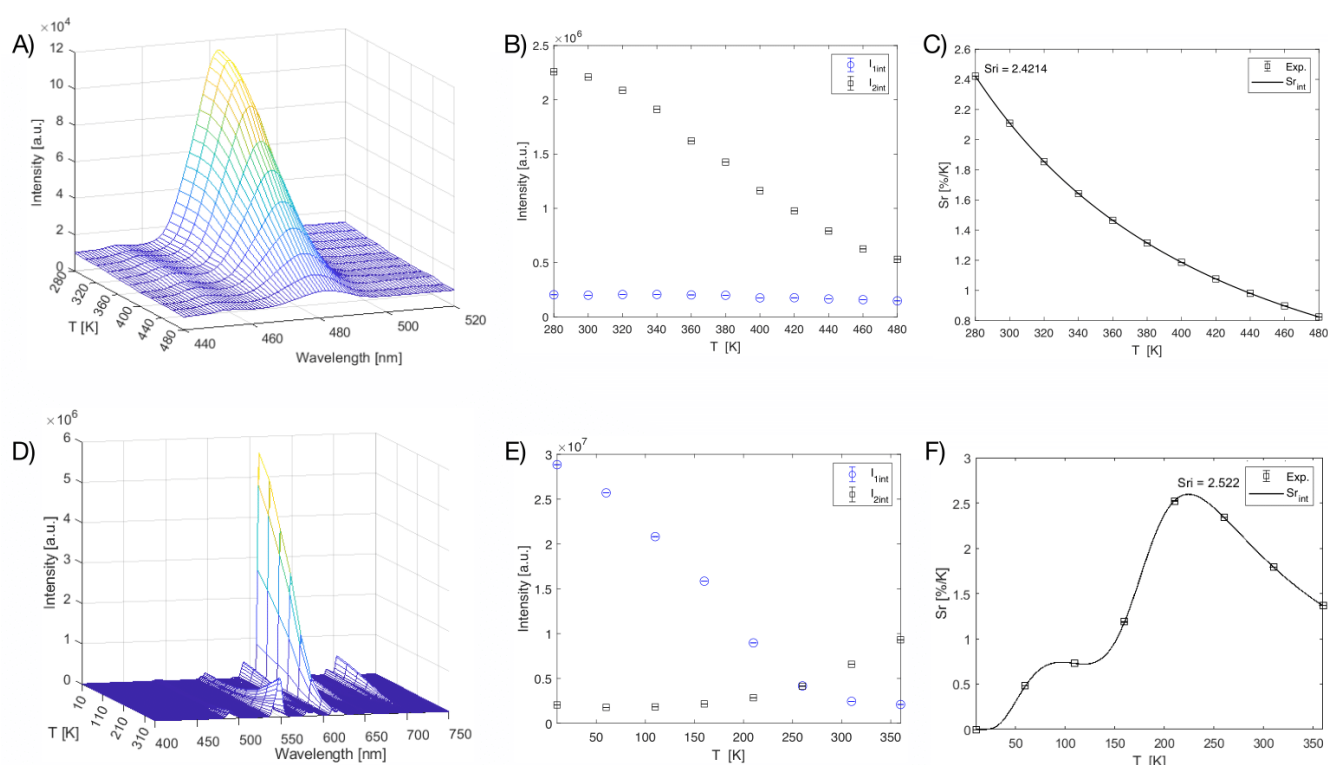
Figure 5. A) Emission map of Dy@Bipy COF recorded at 280-480 K (step 20 K); B) integrated area values for the 455 nm (blue circle) and 483 nm (black square) peaks of Dy@Bipy COF; C) Plot showing the relative sensitivity S_r values at different temperatures for Dy@Bipy COF. The line is meant as a guide to the eye; D) Emission map of 5%Eu,95%Tb@Bipy COF recorded at 10-360 K (step 50 K); E) integrated area values for the 542 nm (black square) and 613 nm (blue circle) peaks of 5%Eu,95%Tb@Bipy COF; F) Plot showing the relative sensitivity S_r values at the different temperatures for 5%Eu,95%Tb@Bipy COF. The line is meant as a guide to the eye.

improves the luminescent efficiency of the material as it works both for shielding the Ln^{3+} ions from water molecules and quenching, as well as a secondary ligand for energy transfer and thus enhances the luminescence signal of the lanthanides grafted onto the COF.

In **Figure S15** the combined excitation-emission spectrum of the optimized Eu@Bipy COF sample is presented. The excitation spectrum consists of a broad band originating from the 3D COF material, while some small, sharp f-f transition peaks, which can be assigned to the Eu^{3+}, are observed. When the compound is excited at 318 nm, the material shows the characteristic $^5D_0 \rightarrow {}^7F_{0-4}$ transition peaks of Eu^{3+}. In **Figure S16** the combined excitation-emission spectrum of Tb@Bipy COF is shown. This material was prepared in a similar way as Eu@Bipy COF, except that $Tb(acac)_3(H_2O)_x$ was used in the synthesis instead of $Eu(acac)_3(H_2O)_x$. The excitation spectrum consists only of a broad band (maximum at 322 nm), which can be assigned to the Bipy COF material itself. This indicates efficient energy transfer from the Bipy COF material to the Tb^{3+} ions. When excited into the ligand band, the characteristic $^5D_4 \rightarrow {}^7F_{6-3}$ transitions peaks of Tb^{3+} are observed.[40]

In **Figure S17** the combined excitation-emission spectrum of Dy@Bipy COF is shown, prepared in a similar way as Eu@Bipy COF and Tb@Bipy COF, however by using the $Dy(acac)_3(H_2O)_x$ complex. As can be noticed, the excitation spectrum consists of a broad band with a maximum at 320 nm. Upon excitation into this broad band the characteristic emission peaks of Dy^{3+} are observed: $^4F_{9/2} \rightarrow {}^6H_{15/2}$ (480 nm), $^4F_{9/2} \rightarrow {}^6H_{13/2}$ (570 nm), and $^4F_{9/2} \rightarrow {}^6H_{11/2}$ (660 nm). This compound was tested for its temperature-dependent luminescence properties to investigate whether it

could potentially be used as a temperature sensor. In general, it is known that Dy^{3+} materials can be used as ratiometric temperature sensors based on the emission from two thermally coupled energy levels by observing the $^4I_{15/2} \rightarrow {}^6H_{15/2}$ and $^4F_{9/2} \rightarrow {}^6H_{15/2}$ transition peaks.[41] The energy difference between the two states is around 900 - 1000 cm^{-1}, which is small enough to reach thermal coupling between the states, but at the same time large enough to ensure well-resolved emission peaks and good sensitivity of the thermometers.[22] The PL properties for this compound were investigated in a temperature range of 280-480 K (steps of 20 K) and are shown in **Figure 5A**. The I_{455}/I_{483} ratio was calculated based on the integrated areas under the peaks (**Figure 5A** and **Figure S18A**). A maximum sensitivity (S_r) of 2.421 %K^{-1} was obtained at 260 K. A good temperature uncertainty δT below 0.055 K for the whole temperature range was obtained (**Figure S18B**). In **Table S1**, the obtained maximum S_r value is compared to some of the few reported Dy^{3+} based temperature sensors.

In a further step, two mixed Eu^{3+},Tb^{3+} hybrid materials were prepared. For this, the complexes were mixed either at 20%Eu,80%Tb or 5%Eu,95%Tb ratio. In **Figure S20** the combined excitation-emission spectrum of 20%Eu,80%Tb@Bipy COF is provided. The spectra were recorded upon exciting at 305 nm and observing at 613 nm. As can be seen the $^5D_4 \rightarrow {}^7F_5$ transition peak (542 nm) of Tb^{3+} is much weaker than the Eu^{3+} transition peaks. The 5%Eu,95%Tb@Bipy COF (excitation spectrum shown in **Figure S21**) showed stronger Tb^{3+} emission intensity than Eu^{3+} emission intensity at room temperature (**Figure 5D**). With temperature increase starting from 10 K it is observed that the Eu^{3+} emission intensity drastically drops,
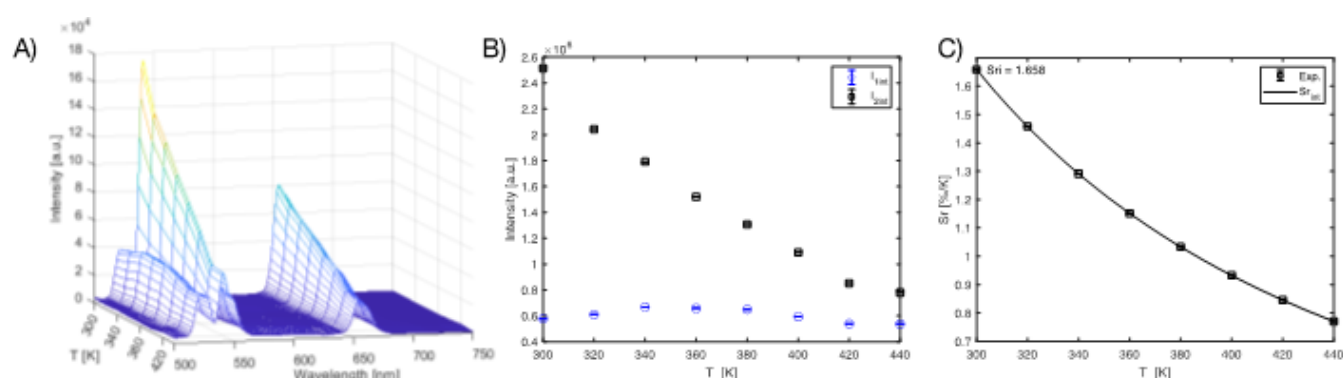
Figure 6. Emission map of NaYF4:Er,Yb@COF-300 recorded at 300-440 K (step 20 K); B) integrated area values for the 523 nm (blue circle) and 543 nm (black square) peaks of NaYF4:Er,Yb@COF-300; C) Plot showing the relative sensitivity S_r values at the different temperatures for NaYF4:Er,Yb@COF-300. The line is meant as a guide to the eye.

whereas the Tb^{3+} emission intensity first remains at the same level and starts to increase around 200-250 K (**Figure 5E**). We have previously observed similar behavior in a reported by some of us Eu,Tb 2D COF[22] and Eu,Tb POP[42] (porous organic polymer). This material was found to be suitable for use as a ratiometric thermometer showing good performance in the 10-360 K temperature range (maximum S_r = 2.522 %K^{-1} at 210 K). The performance of the studied thermometer is compared to other Eu^{3+}/Tb^{3+}@COF systems in **Table S2**. Although good luminescence and thermometric properties can be obtained by grafting lanthanide complexes to Bipy COF, such approach is limited to systems based on one lanthanide ion, which can be grafted to the COF, or a system where two lanthanide ions are in close enough proximity to exhibit energy transfer, or alternatively ones which do not require energy transfer. For example, to develop an UC system based on an Yb-Er lanthanide pair (a Boltzmann type thermometer), the ions need to be in very close proximity to one other and examples of organic based UC systems are very rare.[43] Additionally, the grafting procedure relies on a post-modification procedure using available coordination spots on the COF, limiting the generalizability of this concept. To overcome this problem we have also prepared COF-300, which intentionally lacks available coordination sites for lanthanide grafting, however, as we show can be used in combination with NaYF$_4$:Er,Yb NPs, yielding a NaYF$_4$:Er,Yb@COF-300 nanocomposite material via a one-step process. This way, the inorganic NPs can be doped with any selected lanthanide system and are only then combined with the COF material into a nanocomposite.

The employed here NaYF$_4$:Er,Yb NPs are among the best upconverting materials reported to date.[44] As shown in some of our previous works, upon excitation with a 975 nm continuous wavelength (CW) laser they show three emission peaks: $^2H_{11/2} \rightarrow$ $^4I_{15/2}$ (520 nm), $^4S_{3/2} \rightarrow$ $^4I_{15/2}$ (540 nm) and $^4F_{9/2} \rightarrow$ $^4I_{15/2}$ (650 nm).[45] The two green emission transitions can be used for developing a ratiometric thermometer.[46] In **Figure 6A** we show that this compound possesses good thermometric behavior in the 300-440 K range. The 540 nm peak drops drastically in intensity, whereas the 520 nm peak remains almost at the same intensity throughout the studied temperature range (**Figure 6B**). By taking the ratio of these two peaks we have calculated the Δ parameter (using eqn 1; see **Figure S25**), and further the S_r values. The maximum S_r value could be obtained at 300 K and was calculated to be

1.658 %K^{-1}, which is very good thermometric behavior for a Boltzmann type thermometer.

Conclusion

In this work, 3D COFs were used as ratiometric temperature sensors for the first time. To achieve this, two distinct approaches were employed. In the first route, a bipyridine containing 3D COF was grafted with different lanthanide complexes to obtain Eu@Bipy COF Tb@Bipy COF, Dy@Bipy COF and Eu,Tb@Bipy COF. Even though the porosity of the resulting hybrid materials was strongly reduced, the crystallinity was largely retained, and good thermometric properties could be obtained. Dy@Bipy COF, a rare example of a Dy^{3+} based thermometric system, could be used in the 280-480 K range with maximum sensitivity of S_r = 2.4214 %K^{-1} (260 K) and δT below 0.055 K for the whole temperature range, while 5%Eu,95%Tb@Bipy COF was tested in the 10-360 K temperature range with a maximum S_r of 2.522 %K^{-1} at 210 K. It should be noted that the obtained S_r values are quite high, compared to similar reference materials. In the second route, pre-synthesized NaYF$_4$:Er,Yb NPs were impregnated in a COF without available coordination spots (COF-300) to obtain NaYF$_4$:Er,Yb@COF-300 as a nanocomposite material. This hybrid material was obtained as COF nanocrystallites with the NPs mainly situated on the surface of the COF. It was shown that the crystallinity of both COF and NPs was completely retained during this one-step process, illustrating the superiority of this method from a materials point of view. NaYF$_4$:Er,Yb@COF-300 could be used as a ratiometric temperature sensor in the 300-440 K range with maximum S_r of 1.658 %K^{-1} (300 K). Such a nanocomposite material based on inorganic NPs and a COF material is very attractive, as it allows further using of this concept to implement various luminescence systems, e.g. UC or near-infrared luminescence systems, which are otherwise very difficult to obtain in compounds solely built of organic moieties, and as such extending the possibilities of employing COFs for luminescence applications.

Experimental Section

Synthesis of Bipy COF[33]

30.4 mg TAM and 34 mg 2,2'-bipyridine-5-5'-dicarbaldehyde were collected in a Pyrex® tube and dissolved in a mixture of mesitylene (1.3 mL), phenylmethanol (0.7 mL) and 6 M aqueous acetic acid (0.2 mL). The sample was mixed via ultrasounds, degassed via three pump-thaw cycles, flame sealed and stored in an oven at 120 °C. After 72 hours of reaction time, the formed yellow powder was filtered off, washed with 1,4-dioxane and diethylether and immersed in diethylether over two days. The pure Bipy COF was obtained by filtering this material and treating it in vacuum oven at 80 °C overnight.

Grafting of Ln^{3+} to Bipy COF ($Ln^{3+} = Tb^{3+}$, Eu^{3+}, Dy^{3+})

10 mg Bipy COF and 10/20/40 mg $Ln(acac)_3$·xH_2O (1/2/4 equivalents, respectively) were dissolved in 15 mL ACN and treated in an ultrasound bath until a homogeneous suspension was obtained (2-3 minutes). The vial was sealed and placed in a heating block at 80 °C for 24 h. Afterwards, the materials were filtered off and washed with methanol to remove any ungrafted lanthanide complexes.

Synthesis of $NaYF_4$:Er,Yb@COF-300

The synthesis of $NaYF_4$:Er,Yb@COF-300 was based on the single-crystal synthesis of COF-300, as reported by Wang *et al.*[36] First, two solutions were prepared, solution A contained 268.28 mg terephthalaldehyde (BDA) and 2.413 mL aniline (13.2 eq) in 40 mL 1,4-dioxane, solution **B** consisted of 380.48 mg TAM in 40 mL 1,4-dioxane. Both solutions were sonicated for 5 minutes before being passed through a filter to remove solid particles. Meanwhile, a stock solution of $NaYF_4$:Er,Yb nanoparticles was prepared by dissolving 13 mg of said nanoparticles in 3.25 mL 1,4-dioxane. 2.5 mL of this stock solution was mixed with 4.5 mL of acetic acid and 1.134 mL H_2O and treated with ultrasounds for 5 minutes to obtain solution **C**. Afterwards, in a vial 826 µL of solution **C** was added, followed by 1.4 mL of solution **A**, the resulting solution was treated in the ultrasound bath for 5 minutes. Finally, 1.25 mL of solution **B** was added to the mixture, the samples were gently shaken by hand and stored in a dark room at 20 °C. After ± 3 weeks, leftover reaction liquid was decanted and the $NaYF_4$:Er,Yb@COF-300 was obtained after drying in a vacuum oven at 80 °C.

As a reference, a pure COF-300 material was additionally synthesized following the exact same protocol but with solution **C** consisting purely of 4.5 mL of acetic acid and 1.134 mL H_2O. Therefore, only 576 µL of said solution **C** was used in the synthesis of COF-300.

[1]   A. P. Cote, A. I. Benin, N. W. Ockwig, M. O'Keeffe, A. J. Matzger, O. M. Yaghi, *Science*, **2005**, 310, 1166–1170.

[2]   L. Bourda, C. Krishnaraj, P. Van Der Voort, K. Van Hecke, *Materials Advances* **2021**, *2*, 2811–2845.

[3]   O. M. Yaghi, M. J. Kalmutki, C. S. Diercks in *Introduction to Reticular Chemistry*, Wiley-VCH, Weinheim, Germany, **2019**.

[4]   S. M. J. Rogge, A. Bavykina, J. Hajek, H. Garcia, A. I. Olivos-Suarez, A. Sepúlveda-Escribano, A. Vimont, G. Clet, P. Bazin, F. Kapteijn, et al., *Chemical Society Reviews* **2017**, *46*, 3134–3184.

[5]   D. D. Medina, T. Sick, T. Bein, *Advanced Energy Materials* **2017**, 7, 1700387

[6]   A. Laemont, S. Abednatanzi, P. G. Derakshandeh, F. Verbruggen, E. Fiset, Q. Qin, K. Van Daele, M. Meledina, J. Schmidt, M. Oschatz, P. Van Der Voort, K. Rabaey, M. Antonietti, T. Breugelmans, K. Leus, *Green Chemistry* **2020**, *22*, 3095–3103.

[7]   Y. Zeng, R. Zou, Y. Zhao, *Advanced Materials* **2016**, *28*, 2855–2873.

[8]   C. Krishnaraj, A. M. Kaczmarek, H. S. Jena, K. Leus, N. Chaoui, J. Schmidt, R. Van Deun, P. Van Der Voort, *ACS Applied Materials & Interfaces* **2019**, *11*, 27343–27352.

[9]   C. Krishnaraj, H. Sekhar Jena, L. Bourda, A. Laemont, P. Pachfule, J. Roeser, C. V. Chandran, S. Borgmans, S. M. J. Rogge, K. Leus, C. V. Stevens, J. A. Martens, V. Van Speybroeck, E. Breynaert, A. Thomas, P. Van Der Voort, *Journal of the American Chemical Society* **2020**, *142*, 20107–20116.

[10]   H. S. Jena, C. Krishnaraj, G. Wang, K. Leus, J. Schmidt, N. Chaoui, P. Van Der Voort, P., *Chem. Mater.* **2018**, 30, 4102,

[11]   Q. Fang, J. Wang, S. Gu, R. B. Kaspar, Z. Zhuang, J. Zheng, H. Guo, S. Qiu, Y. Yan, *Journal of the American Chemical Society* **2015**, *137*, 8352–8355.

[12]   X. Guan, F. Chen, Q. Fang, S. Qiu, *Chemical Society Reviews* **2020**, *49*, 1357–1384.

[13]   L. A. Baldwin, J. W. Crowe, D. A. Pyles, P. L. Mcgrier, *Journal of the American Chemical Society* **2016**, *138*, 15134–15137.

[14]   S. Yan, X. Guan, H. Li, D. Li, M. Xue, Y. Yan, V. Valtchev, S. Qiu, Q. Fang, *Journal of the American Chemical Society* **2019**, *141*, 2920–2924.

[15]   W. Gao, X. Sun, H. Niu, X. Song, K. Li, H. Gao, W. Zhang, J. Yu, M. Jia, *Microporous Mesoporous Mater.*, **2015**, 213, 59–67.

[16]   Y. Xin, C. Wang, Y. Wang, J. Sun, Y. Gao, *RSC Advances* **2017**, *7*, 1697–1700.

[17]   J.-C. G. Bünzli, C. Piguet, *Chem. Soc. Rev.* 2005, **34**, 1048.

[18]   J.-C. G. Bünzli, *Acc. Chem. Res.* **2006**, *39*, 53.

[19]   J. Rocha, C. D. S. Brites, L. D. Carlos, *Chemistry – A European Journal* **2016**, *22*, 14782–14795.

[20]   A. M. Kaczmarek, *Journal of Materials Chemistry C* **2018**, *6*, 5916–5925.

[21]   L. Bourda, H. S. Jena, R. Van Deun, A. M. Kaczmarek, P. Van Der Voort, *Journal of Materials Chemistry A* **2019**, *7*, 14060–14069.

[22]   A. M. Kaczmarek, Y. Liu, M. K. Kaczmarek, H. Liu, F. Artizzu, L. D. Carlos, P. Van Der Voort, *Angewandte Chemie International Edition* **2020**, *59*, 1932–1940.

[23]   A. M. Kaczmarek, H. S. Jena, C. Krishnaraj, H. Rijckaert, S. K. P. Veerapandian, A. Meijerink, P. Van Der Voort, *Angewandte Chemie International Edition* **2021**, *60*, 3727–3736.

[24]   P. Gohari Derakhshandeh, S. Abednatanzi, L. Bourda, S. Dalapati, A. Abalymov, M. Meledina, Y.-Y. Liu, A. G. Skirtach, K. Van Hecke, A. M. Kaczmarek, et al., *Journal of Materials Chemistry C* **2021**, *9*, 6436–6444.

[25]   C. Krishnaraj, H. Rijckaert, H. S. Jena, P. Van Der Voort, A. M. Kaczmarek, *ACS Applied Materials & Interfaces* **2021**, *13*, 47010–47018.

[26]   S. Premcheska, M. Lederer, A. M. Kaczmarek, *Chemical Communications* **2022**, DOI 10.1039/d1cc07164e.

[27]   H. S. Jena, H. Rijckaert, C. Krishnaraj, I. Van Driessche, P. Van Der Voort, A. M. Kaczmarek, *Chemistry of Materials* **2021**, *33*, 8007–8017.

[28]   C. D. S. Brites, S. Balabhadra, L. D. Carlos, *Advanced Optical Materials* **2019**, *7*, 1801239.

[29] R. G. Geitenbeek, A.-E. Nieuwelink, T. S. Jacobs, B. B. V. Salzmann, J. Goetze, A. Meijerink, B. M. Weckhuysen, *ACS Catalysis* **2018**, *8*, 2397–2401.

[30] T. P. Van Swieten, T. Van Omme, D. J. Van Den Heuvel, S. J. W. Vonk, R. G. Spruit, F. Meirer, H. H. P. Garza, B. M. Weckhuysen, A. Meijerink, F. T. Rabouw, et al., *ACS Applied Nano Materials* **2021**, *4*, 4208–4215.

[31] W.-K. Li, P. Ren, Y.-W. Zhou, J.-T. Feng, Z.-Q. Ma, *Journal of Hazardous Materials* **2020**, 388 , art. no. 121740.

[32] Q. Sun, C. Wu, Q. Pan, B. Zhang, Y. Liu, X. Lu, J. Sun, L. Sun, Y. Zhao, *ChemNanoMat* **2021**, *7*, 95–99.

[33] H. Rijckaert, S. Premcheska, S. Mohanty, J. Verduijn, A. Skirtach, A. M. Kaczmarek, *Physica B, Condensed Matter* **2022**, 626, 413453.

[34] A. M. Kaczmarek, M. Suta, H. Rijckaert, A. Abalymov, I. Van Driessche, A. G. Skirtach, A. Meijerink, P. Van Der Voort, *Advanced Functional Materials* **2020**, *30*, 2003101.

[35] J. Sun, H. Rijckaert, Y. Maegawa, S. Inagaki, P. Van Der Voort, A. M. Kaczmarek, *Chemistry of Materials* **2022**, *34*, 3770–3780.

[36] X. Wang, R. Enomoto, Y. Murakami, *Chemical Communications* **2021**, *57*, 6656–6659.

[37] T. Ma, E. A. Kapustin, S. X. Yin, L. Liang, Z. Zhou, J. Niu, L.-H. Li, Y. Wang, J. Su, J. Li, et al., *Science* **2018**, *361*, 48–52.

[38] A. Grzechnik, P. Bouvier, M. Mezouar, M. D. Mathews, A. K. Tyagi, J. Köhler, *Journal of Solid State Chemistry* **2002**, 165, 159-164.

[39] K. Binnemans, *Coordination Chemistry Reviews* **2015**, *295*, 1–45.

[40] H. S. Jena, A. M. Kaczmarek, C. Krishnaraj, X. Feng, K. Vijayvergia, H. Yildirim, S.-N. Zhao, R. Van Deun, P. V. Der Voort, *Crystal Growth & Design* **2019**, *19*, 6339–6350.

[41] A. M. Kaczmarek, *Journal of Materials Chemistry C* **2018**, *6*, 5916–5925.

[42] F. Vanden Bussche, A. M. Kaczmarek, S. K. P. Veerapandian, J. Everaert, M. Debruyne, S. Abednatanzi, R. Morent, N. De Geyter, V. Van Speybroeck, P. Van Der Voort, et al., *Chemistry – A European Journal* **2020**, *26*, 15596–15604.

[43] F. Artizzu, F. Quochi, L. Marchiò, E. Sessini, M. Saba, A. Serpe, A. Mura, M. L. Mercuri, G. Bongiovanni, P. Deplano, *The Journal of Physical Chemistry Letters* **2013**, *4*, 3062–3066.

[44] C. Homann, L. Krukewitt, F. Frenzel, B. Grauel, C. Würth, U. Resch-Genger, M. Haase, *Angewandte Chemie International Edition* **2018**, *57*, 8765–8769.

[45] A. M. Kaczmarek, M. Suta, H. Rijckaert, T. P. Van Swieten, I. Van Driessche, M. K. Kaczmarek, A. Meijerink, *Journal of Materials Chemistry C* **2021**, *9*, 3589–3600.

[46] R. G. Geitenbeek, P. T. Prins, W. Albrecht, A. Van Blaaderen, B. M. Weckhuysen, A. Meijerink, *The Journal of Physical Chemistry C* **2017**, *121*, 3503–3510.

Entry for the Table of Contents

Insert graphic for Table of Contents here. ((Please ensure your graphic is in **one** of following formats))

((max. width: 5.5 cm; max. height: 5.0 cm))

Please delete this box prior to submission

((max. width: 11.5 cm; max. height: 2.5 cm))

Please delete this box prior to submission

Two routes to develop hybrid Ln@3D COF materials were studied. A bipyridine-containing 3D COF was grafted with a range of visible emitting lanthanide complexes, while a novel nanocomposite material was prepared by impregnating a 3D COF without available coordination sites with upconverting $NaYF_4$:Er,Yb nanoparticles. The obtained materials were tested as luminescent ratiometric temperature sensors.

((The Table of Contents text should give readers a short preview of the main theme of the research and results included in the paper to attract their attention into reading the paper in full. The Table of Contents text **should be different from the abstract** and should be no more than 50-60 words long.))

Institute and/or researcher Twitter usernames: ((optional))